

## Effective Hamiltonian and unitarity of the $S$ matrix

I. Rotter

*Max-Planck-Institut für Physik komplexer Systeme, D-01187 Dresden, Germany*

(Received 27 February 2003; published 15 July 2003)

The properties of open quantum systems are described well by an effective Hamiltonian  $\mathcal{H}$  that consists of two parts: the Hamiltonian  $H$  of the closed system with discrete eigenstates and the coupling matrix  $W$  between discrete states and continuum. The eigenvalues of  $\mathcal{H}$  determine the poles of the  $S$  matrix. The coupling matrix elements  $\tilde{W}_k^{cc'}$  between the eigenstates  $k$  of  $\mathcal{H}$  and the continuum may be very different from the coupling matrix elements  $W_k^{cc'}$  between the eigenstates of  $H$  and the continuum. Due to the unitarity of the  $S$  matrix, the  $\tilde{W}_k^{cc'}$  depend on energy in a nontrivial manner. This conflicts with the assumptions of some approaches to reactions in the overlapping regime. Explicit expressions for the wave functions of the resonance states and for their phases in the neighborhood of, respectively, avoided level crossings in the complex plane and double poles of the  $S$  matrix are given.

DOI: 10.1103/PhysRevE.68.016211

PACS number(s): 73.21.La, 72.15.Qm, 03.65.Nk, 03.65.Vf

### I. INTRODUCTION

Quantum systems are characterized by a number of discrete states the structure of which is more or less complicated. These quantum systems do, however, not exist isolated from other systems. Most of them are embedded in an environment, e.g., in the continuum of decay channels. System and environment interact with one another, and it is this interaction that allows us to study the properties of the system. The feedback of the interaction with the environment onto the properties of the system itself is an old problem raised in the very beginning of the quantum mechanics. It becomes the more important the smaller the system is.

As an example, most states of a nucleus are embedded in the continuum of decay channels due to which they get a finite lifetime. In other words, the discrete states of a nucleus shade off into resonance states with complex energies  $\mathcal{E}_k = E_k - (i/2)\Gamma_k$ . The values  $E_k$  give the positions in energy of the resonance states, while the widths  $\Gamma_k$  are characteristic of their lifetimes. The values  $E_k$  may be different from the energies of the discrete states, and the widths  $\Gamma_k$  may be large corresponding to a short lifetime. Nevertheless, there is a well-defined relation between the discrete states characterizing the closed system and the resonance states appearing in the open system. The main difference in the theoretical description of quantum systems without and with coupling to an environment is that the function space of the system is supposed to be complete in the first case, while this is not so in the second case. Accordingly, the Hamilton operator is Hermitian in the first case, and the eigenvalues are discrete. The resonance states, however, characterize a subsystem described by a non-Hermitian Hamilton operator with complex eigenvalues. The function space containing everything consists, in the second case, of system plus environment.

The mathematical formulation of this problem goes back to Feshbach [1] who introduced the two subspaces  $Q$  and  $P$ , with  $Q + P = 1$ , containing the discrete and scattering states, respectively. Feshbach was able to formulate a unified description of nuclear reactions with direct processes in the short-time scale and compound nucleus processes in the

long-time scale. Due to the high excitation energy and high level density in compound nuclei, he introduced statistical approximations in order to describe the discrete states of the  $Q$  subspace. A unified description of nuclear structure and nuclear reaction aspects is much more complicated and became possible only at the end of the last century (see Ref. [2] for a recent review). In this formulation, the states of both subspaces are described with the same accuracy. All the coupling matrix elements between different discrete states, different scattering states as well as between discrete and scattering states have to be calculated in order to get results that can be compared with the experimental data. This method has been applied to the description of light nuclei by using the shell model approach for the discrete many-particle states of the  $Q$  subspace [2].

In the unified description of structure and reaction aspects, the system is described by an effective Hamiltonian  $\mathcal{H}$  that consists of two terms: the Hamiltonian matrix  $H$  of the closed system with discrete eigenstates, and the coupling matrix between system and environment. The last term is responsible for the finite lifetime of the resonance states. The eigenvalues of  $\mathcal{H}$  are complex and give the poles of the  $S$  matrix. The motion of these eigenvalues as a function of a certain parameter is discussed in many papers (see for the recent review Ref. [2]). The statistics of complex eigenvalues and the corresponding nonorthogonal eigenvectors for non-Hermitian random matrices are recently considered in Ref. [3].

The coupling matrix elements  $\tilde{W}_k^{cc'}$  between the resonance states and the continuum are seldom studied. Their relation to the coupling matrix elements  $W_k^{cc'}$  between the corresponding discrete states and the continuum can be expressed by the mixing coefficients that appear in the representation of the wave functions of the resonance states in the set of wave functions of the discrete states. Generically, the relation between the wave functions of the resonance states and those of the discrete states is complicated since the number of discrete states of a realistic system is large. Many of them can contribute to the wave function of a certain resonance state, almost independently of their energetical dis-

tance, see, e.g., Ref. [4]. The numerical results for the coupling matrix elements  $\tilde{W}_k^{cc'}$  of nuclear states show a nontrivial energy dependence, especially at high level density [2]. In the statistical approach to nuclear reactions and the application of this approach to some other reactions, they are, however, assumed to be simple, energy-independent parameters such as the  $W_k^{cc'}$ , e.g., Refs. [5–9].

The aim of the present paper is (i) to study the energy dependence of the coupling matrix elements  $\tilde{W}_k^{cc'}$  between resonance states and continuum that follows immediately from the unitarity of the  $S$  matrix, and (ii) to study the behavior of the wave functions of the resonance states in the overlapping regime since these determine the energy dependence of the  $\tilde{W}_k^{cc'}$  in numerical calculations performed for special systems. Most interesting is the behavior of the wave functions near avoided level crossings in the complex plane.

As the results show, the coupling coefficients  $\tilde{W}_k^{cc'}$  are, generically, energy dependent. The energy dependence is, however, not important as long as the distance in energy between the resonance states is larger than the sum of their widths. This result is in full agreement with the statement of the authors of the review [5] who restricted the application of their approach to the nonoverlapping regime. In the overlapping regime, however, the energy dependence of the coupling coefficients  $\tilde{W}_k^{cc'}$  cannot be neglected. It follows from the unitarity of the  $S$  matrix and causes nonlinear terms in the  $S$  matrix at high level density. Nevertheless, the line shape of the resonances can equivalently be described by the energy independent  $W_k^{cc'}$  in many cases. The  $W_k^{cc'}$  lose, however, their physical meaning in the overlapping regime [10]. As to the wave functions of two resonance states  $k$  and  $l$  in the neighborhood of an avoided level crossing in the complex plane, these are mixed:  $\beta_k \tilde{\Phi}_k \pm i \beta_l \tilde{\Phi}_l$ . The corresponding phase changes in approaching the critical value of the parameter at which the levels avoid crossing (where  $\beta_k = \pm \beta_l$ ) are caused by nonlinear terms in the Schrödinger equation. These terms are, finally, responsible for the energy dependence of the coupling coefficients  $\tilde{W}_k^{cc'}$  between system and continuum in numerical calculations. This result following from the behavior of the wave functions of the resonance states at high level density coincides with that following from the unitarity of the  $S$  matrix.

The paper is organized in the following manner. In Sec. II, the main ingredients of the unified description of structure and reaction aspects of a quantum system embedded in a continuum are given. These are the effective Hamiltonian  $\mathcal{H}$  of the system and the  $S$  matrix. Both are derived by solving the Schrödinger equation in the full function space with discrete and continuous states. Further, some properties of the spectroscopic values that characterize the system are sketched with special emphasis of their behavior in the overlapping regime. In Sec. III, the coupling coefficients  $\tilde{W}$  between system and continuum are directly obtained in the one-channel case by starting from a unitary  $S$  matrix. The nonlinear effects appearing in the overlapping regime are discussed. The wave functions at avoided level crossings in

the complex plane and in its neighborhood are derived in Sec. IV. They are energy dependent and their phases change in a certain range around the critical value of the parameter at which the resonance states avoid crossing. Section V contains concluding remarks on the energy dependence of the coupling coefficients  $\tilde{W}_k^{cc'}$  appearing in a model with a unified description of structure and reaction aspects at high level density.

## II. EFFECTIVE HAMILTONIAN AND $S$ MATRIX FOR A QUANTUM SYSTEM EMBEDDED IN A CONTINUUM

In the unified description of structure and reaction aspects of quantum systems, the Schrödinger equation

$$(H^{\text{full}} - E)\Psi(E) = 0 \quad (1)$$

is solved in a function space containing everything, i.e., discrete as well as continuous states. The Hamilton operator  $H^{\text{full}}$  is Hermitian, the wave functions  $\Psi$  depend on energy as well as on the decay channels and all the resonance states of the system. Knowing the wave functions  $\Psi(E)$ , an expression for the  $S$  matrix can be derived which holds true also in the overlapping regime, see the recent review [2]. It reads

$$S_{cc'} = e^{i(\delta_c - \delta_{c'})} [\delta_{cc'} - S_{cc'}^{(1)} - S_{cc'}^{(2)}], \quad (2)$$

where  $\delta_c$  is the phase shift in channel  $c$ ,  $S_{cc'}^{(1)}$  is the smooth direct reaction part related to the short-time scale, and

$$S_{cc'}^{(2)} = i \sum_{k=1}^N \frac{\tilde{\gamma}_k^c \tilde{\gamma}_k^{c'}}{E - \tilde{E}_k + \frac{i}{2} \tilde{\Gamma}_k} \quad (3)$$

is the resonance reaction part related to the long-time scale. Here, the  $\tilde{\mathcal{E}}_k = \tilde{E}_k - (i/2)\tilde{\Gamma}_k$  are the complex energy dependent eigenvalues of the non-Hermitian Hamilton operator

$$\mathcal{H} \equiv \mathcal{H}_{QQ} = H_{QQ} + H_{QP} G_P^{(+)} H_{PQ} \quad (4)$$

appearing effectively in the system ( $Q$  subspace) after embedding it into the continuum ( $P$  subspace). It is  $H^{\text{full}} \equiv H_{QQ} + H_{QP} + H_{PQ} + H_{PP}$  where  $H_{QQ}$  is the Hamiltonian of the closed system and  $H_{PP}$  is that for the environment (scattering states). The two terms  $H_{PQ}$  and  $H_{QP}$  characterize the coupling between the two subspaces. These two terms appear in the source terms of the equations in either subspace when  $Q + P = 1$  as well as in the effective Hamiltonians of the subspaces. The effective Hamiltonian in the  $Q$  subspace is given in Eq. (4), and an analogous expression for the effective Hamiltonian in the  $P$  subspace can be written down, see Ref. [2]. Usually,  $\text{Re}(H_{QP} G_P^{(+)} H_{PQ}) \neq 0$  and  $\text{Re}(\mathcal{H}) \equiv H_{QQ} + \text{Re}(H_{QP} G_P^{(+)} H_{PQ}) \neq H_{QQ}$ , see Ref. [2] for a detailed discussion. The  $G_P^{(+)}$  in Eq. (4) are the Green functions in the  $P$  subspace, and  $\text{Im}(H_{QP} G_P^{(+)} H_{PQ})$  is determined by the coupling matrix elements

$$\tilde{\gamma}_k^c = \sqrt{2\pi} \langle \xi_E^c | V | \tilde{\Phi}_k \rangle \quad (5)$$

between the resonance states and the scattering states. The  $\tilde{\gamma}_k^c$  are complex and also energy-dependent functions. In Eq. (5), the  $\xi_E^c$  are the scattering wave functions and the  $\tilde{\Phi}_k$  are the eigenfunctions of  $\mathcal{H}$ , Eq. (4). The wave functions  $\tilde{\Omega}_k$  of the resonance states are related to the eigenfunctions  $\tilde{\Phi}_k$  of  $\mathcal{H}$  by a Lippmann-Schwinger-like relation [2],

$$\tilde{\Omega}_k = (1 + G_P^{(+)} H_{PQ}) \tilde{\Phi}_k. \quad (6)$$

The eigenfunctions of  $\mathcal{H}$  are biorthogonal,

$$\langle \tilde{\Phi}_l^* | \tilde{\Phi}_k \rangle = \delta_{kl}, \quad (7)$$

so that

$$\langle \tilde{\Phi}_k | \tilde{\Phi}_k \rangle = \text{Re}(\langle \tilde{\Phi}_k | \tilde{\Phi}_k \rangle); \quad A_k \equiv \langle \tilde{\Phi}_k | \tilde{\Phi}_k \rangle \geq 1 \quad (8)$$

and

$$\langle \tilde{\Phi}_k | \tilde{\Phi}_{l \neq k} \rangle = i \text{Im}(\langle \tilde{\Phi}_k | \tilde{\Phi}_{l \neq k} \rangle) = -\langle \tilde{\Phi}_{l \neq k} | \tilde{\Phi}_k \rangle;$$

$$B_k^{l \neq k} \equiv |\langle \tilde{\Phi}_k | \tilde{\Phi}_{l \neq k} \rangle| \geq 0. \quad (9)$$

It should be noticed that the standard normalization  $\langle \tilde{\Phi}_l | \tilde{\Phi}_k \rangle = \delta_{kl}$  is equivalent to Eqs. (7)–(9) for all  $k, l$  but those with  $\tilde{\mathcal{E}}_k = \tilde{\mathcal{E}}_l$  (double pole of the  $S$  matrix) where  $A_k \rightarrow \infty$  and  $B_k^l \rightarrow \infty$ . As a consequence of Eq. (8) holds [2]

$$\tilde{\Gamma}_k = \frac{\sum_c |\tilde{\gamma}_k^c|^2}{A_k} \leq \sum_c |\tilde{\gamma}_k^c|^2. \quad (10)$$

The main difference to the standard theory is that the  $\tilde{\gamma}_k$ ,  $\tilde{\Gamma}_k$ , and  $\tilde{E}_k$  are not numbers but energy-dependent functions [2]. The energy dependence of  $\text{Im}\{\tilde{\mathcal{E}}_k\} = -\frac{1}{2}\tilde{\Gamma}_k$  is large near to the threshold for opening the first decay channel. This causes not only deviations from the Breit Wigner line shape of isolated resonances lying near to the threshold but also an interference with the above-threshold “tail” of bound states [2]. Also, an inelastic threshold may have an influence on the line shape of a resonance when the resonance lies near to the threshold and is coupled strongly to the channel which opens [11]. Also, in this case,  $\tilde{\Gamma}_k$  depends strongly on energy. In the cross section, a cusp may appear in the cross section instead of a resonance of Breit Wigner shape. Both types of threshold effects in the line shape of resonances can explain experimental data known in nuclear physics [2]. They cannot be simulated by a parameter in the  $S$  matrix.

The energy dependence of  $\tilde{E}_k$  and  $\tilde{\Gamma}_k$  may be important also far from decay thresholds [2]. Characteristic of the mo-

tion of the poles of the  $S$  matrix as a function of a certain parameter (which may be also the energy  $E$  of the system) are the following generic results obtained for very different systems in the overlapping regime: the trajectories of the  $S$  matrix poles avoid crossing with the only exception of exact crossing when the  $S$  matrix has a double (or multiple) pole. At the avoided crossing, either level repulsion or level attraction occurs. The first case is caused by a predominantly real interaction between the crossing states and is accompanied by the tendency to form a uniform time scale of the system. Level attraction occurs, however, when the interaction is dominated by its imaginary part arising from the coupling via the continuum. It is accompanied by the formation of different time scales in the system: while some of the states decouple more or less completely from the continuum and become long-lived (trapped), a few of the states become short-lived and wrap the long-lived ones in the cross section. The dynamics of quantum systems at high level density is determined by the interplay of these two opposite tendencies. For a more detailed discussion, see Ref. [2].

One of these tendencies, the phenomenon of resonance trapping

$$\sum_{k=1}^N \tilde{\Gamma}_k \approx \sum_{K=1}^K \tilde{\Gamma}_k; \quad \sum_{k=K+1}^N \tilde{\Gamma}_k \approx 0, \quad (11)$$

appears only in the overlapping regime. It is caused by  $\text{Im}(\mathcal{H})$  and means almost complete decoupling of  $N-K$  resonance states from the continuum, while  $K$  of them become short-lived [2]. Usually,  $K \ll N-K$ . The long-lived resonance states in the overlapping regime appear often to be well isolated from one another [10]. The few short-lived resonance states determine the evolution of the system. This means, quick direct reaction processes may appear, at large overall coupling strength, from slow resonance processes by means of the resonance trapping phenomenon. Meanwhile, the phenomenon of resonance trapping has been proven experimentally on a microwave cavity as a function of the degree of opening of the cavity to an attached lead [12]. In this experiment, the varied parameter is the overall coupling strength between discrete and scattering states. Resonance trapping may appear, however, as a function of any parameter [2].

In any case, the energies and widths of the resonance states follow from the solutions of the fixed-point equations:

$$E_k = \tilde{E}_k(E = E_k) \quad \text{and} \quad \Gamma_k = \tilde{\Gamma}_k(E = E_k), \quad (12)$$

on condition that the two subspaces are defined adequately [2]. The values  $E_k$  and  $\Gamma_k$  correspond to the standard spectroscopic observables. The wave functions of the resonance states are defined by the functions  $\tilde{\Omega}_k$ , Eq. (6), at the energy  $E = E_k$ . The partial widths are related to the coupling matrix elements  $(\tilde{\gamma}_k^c)^2$  that are calculated independently by means of the eigenfunctions  $\tilde{\Phi}_k$  of  $\mathcal{H}$ . For isolated resonances,  $A_k = 1$  according to Eq. (8), and the standard relation  $\Gamma_k = \sum_c |\tilde{\gamma}_k^c|^2$  follows from Eq. (10). In the overlapping regime,

the partial widths lose their physical meaning, since  $A > 1$ . Both functions  $(\tilde{\gamma}_k^c)^2$  and  $\tilde{\Gamma}_k$  may even show a different energy dependence [2].

It follows immediately from Eq. (4) that the coupling of the resonance states via the continuum induces additional correlations between the states. These correlations are described by the term  $H_{QP}G_P^{(+)}H_{PQ}$  of the effective Hamiltonian  $\mathcal{H}$ . The real part  $\text{Re}(H_{QP}G_P^{(+)}H_{PQ})$  causes level repulsion in energy and is accompanied by the tendency to form a uniform time scale in the system. In contrast to this behavior, the imaginary part  $\text{Im}(H_{QP}G_P^{(+)}H_{PQ})$  causes different time scales in the system and is accompanied by level attraction in energy. Thus, an essential part of the energy dependence of the eigenvalues of  $\mathcal{H}$  is caused by the additional correlations of the states via the continuum. These are important, above all, at high level density.

For isolated resonance states, the additional shift in energy is usually taken into account by simulating  $\text{Re}(\mathcal{H}) = H_{QQ} + \text{Re}(H_{QP}G_P^{(+)}H_{PQ})$  by  $H_0 + V'$ , where  $V'$  is assumed to be describable by two-body effective residual forces. It should be mentioned, however, that  $\text{Re}(H_{QP}G_P^{(+)}H_{PQ})$  cannot be completely simulated by an additional contribution to the residual two-body interaction even in the case of well-isolated resonances, since it contains many-body effects, as follows from the analytical structure of  $H_{QP}G_P^{(+)}H_{PQ}$ .  $\text{Re}(H_{QP}G_P^{(+)}H_{PQ})$  is an integral over energy and depends explicitly on the energies  $\epsilon_c$  at which the channels  $c$  open. For details, see Ref. [2].

Spectroscopic studies in the overlapping regime are more complicated. The wave functions  $\tilde{\Phi}_k$  may be represented in the set of eigenfunctions  $\{\Phi_k\}$  of the Hermitian Hamilton operator  $H \equiv H_{QQ}$ ,

$$\tilde{\Phi}_k = \sum_l b_{kl} \Phi_l. \quad (13)$$

The  $\Phi_k$  are real, while the  $\tilde{\Phi}_k$  are complex and energy dependent in the overlapping regime. The coefficients  $b_{kl}$  and the  $\tilde{\gamma}_k^c$  are complex and energy dependent, too. In this regime, the differences between  $\mathcal{H}$  and  $H$  therefore cannot be simulated in a simple manner. Even the positions of the peaks in the cross section do, generally, not appear at the energies  $E_k$  when the resonance states overlap [2]. This is the result of interferences between the resonance states.

It should be underlined here that expression (3) for the resonance reaction part of the  $S$  matrix is derived from the Schrödinger equation (1) by rewriting it in a consistent manner. Here, the eigenvalues  $\tilde{\mathcal{E}}_k = \tilde{E}_k - (i/2)\tilde{\Gamma}_k$  of the effective Hamiltonian  $\mathcal{H}$ , Eq. (4), as well as the coupling matrix elements  $\tilde{\gamma}_k^c$ , are energy-dependent functions, and the unitarity of the  $S$  matrix is guaranteed.

Furthermore, the different  $\tilde{\Phi}_k (E = E_k)$  are neither strictly orthogonal nor biorthogonal since the biorthogonality relation (7) holds only when the energies of both states  $k$  and  $l$  are equal. The spectroscopic studies on resonance states are performed, therefore, with the wave functions being only

approximately biorthogonal. The deviations from the biorthogonality relation (7) are, however, small as a rule. This drawback of the spectroscopic studies of resonance states has to be contrasted with the advantage it has for the study of observable values: the  $S$  matrix and therefore the cross section are calculated with the resonance wave functions being strictly biorthogonal at every energy  $E$  of the system. Furthermore, the full energy dependence of  $\tilde{E}_k, \tilde{\Gamma}_k$  and, above all, of the coupling matrix elements  $\tilde{\gamma}_k^c$  is taken into account in the  $S$  matrix and therefore in all calculations for observable values.

### III. UNITARITY OF THE $S$ MATRIX

The Breit Wigner one-level formula for nuclear reactions describes the reaction cross section with isolated resonances. The  $S$  matrix elements for this case read

$$S_{cc'} = 1 - i \sum_k \frac{\tilde{W}_k^{cc'}}{E - \tilde{E}_k + \frac{i}{2} \tilde{\Gamma}_k}, \quad (14)$$

where  $\tilde{E}_k$  and  $\tilde{\Gamma}_k$  are the energies and widths of the resonance states  $k$ , respectively, and  $\tilde{W}_k^{cc'} \equiv \tilde{\gamma}_k^c \tilde{\gamma}_k^{c'}$ . The  $\tilde{\gamma}_k^c$  are the partial widths of the states  $k$  relative to the channel  $c$ . The values  $\tilde{E}_k, \tilde{\Gamma}_k$ , and  $\tilde{\gamma}_k^c$  are numbers characterizing the properties of the resonance states  $k$ . Since they are energy-independent values, the decay follows an exponential law.

For an isolated resonance state  $k=1$  coupled to one channel,

$$S = 1 - i \frac{\tilde{W}_1}{E - \tilde{E}_1 + \frac{i}{2} \tilde{\Gamma}_1} \quad (15)$$

in the energy range  $\tilde{E}_1 - \frac{1}{2}\tilde{\Gamma}_1 \leq E \leq \tilde{E}_1 + \frac{1}{2}\tilde{\Gamma}_1$ , and  $\tilde{W}_1 = \tilde{\Gamma}_1$  due to the unitarity of the  $S$  matrix. The last relation follows immediately from Eq. (15) that, in the one-resonance-one-channel case, can be written as

$$S = \frac{E - \tilde{E}_1 - \frac{i}{2} \tilde{\Gamma}_1}{E - \tilde{E}_1 + \frac{i}{2} \tilde{\Gamma}_1} \quad (16)$$

when  $\tilde{W}_1 = \tilde{\Gamma}_1$ . The  $S$  matrix (16) is unitary.

Let us now consider the unitary representation of the  $S$  matrix in the one-channel case with two resonance states,

$$S = \frac{\begin{pmatrix} E - \tilde{E}_1 - \frac{i}{2} \tilde{\Gamma}_1 \\ E - \tilde{E}_2 - \frac{i}{2} \tilde{\Gamma}_2 \end{pmatrix}}{\begin{pmatrix} E - \tilde{E}_1 + \frac{i}{2} \tilde{\Gamma}_1 \\ E - \tilde{E}_2 + \frac{i}{2} \tilde{\Gamma}_2 \end{pmatrix}}. \quad (17)$$

From this expression, a possible form of the pole representation of the  $S$  matrix can be derived,

$$\begin{aligned}
S &= 1 - \frac{i\tilde{\Gamma}_1}{E - \tilde{E}_1 + \frac{i}{2}\tilde{\Gamma}_1} - \frac{i\tilde{\Gamma}_2}{E - \tilde{E}_2 + \frac{i}{2}\tilde{\Gamma}_2} - \frac{\tilde{\Gamma}_1\tilde{\Gamma}_2}{\left(E - \tilde{E}_1 + \frac{i}{2}\tilde{\Gamma}_1\right)\left(E - \tilde{E}_2 + \frac{i}{2}\tilde{\Gamma}_2\right)} \\
&= 1 - \frac{1}{E - \tilde{E}_1 + \frac{i}{2}\tilde{\Gamma}_1} \left( i\tilde{\Gamma}_1 + \frac{\tilde{\Gamma}_1\tilde{\Gamma}_2}{2E - (\tilde{E}_1 + \tilde{E}_2) + \frac{i}{2}(\tilde{\Gamma}_1 + \tilde{\Gamma}_2)} \right) \\
&\quad - \frac{1}{E - \tilde{E}_2 + \frac{i}{2}\tilde{\Gamma}_2} \left( i\tilde{\Gamma}_2 + \frac{\tilde{\Gamma}_1\tilde{\Gamma}_2}{2E - (\tilde{E}_1 + \tilde{E}_2) + \frac{i}{2}(\tilde{\Gamma}_1 + \tilde{\Gamma}_2)} \right). \tag{18}
\end{aligned}$$

It follows

$$S = 1 - i \sum_{k=1,2} \frac{\tilde{W}_k}{E - \tilde{E}_k + \frac{i}{2}\tilde{\Gamma}_k}, \tag{19}$$

in complete analogy to Eq. (14), with

$$\tilde{W}_k = \tilde{\Gamma}_k \left( 1 - i \frac{\tilde{\Gamma}_l}{2E - (\tilde{E}_k + \tilde{E}_l) + \frac{i}{2}(\tilde{\gamma}_k + \tilde{\Gamma}_l)} \right) \tag{20}$$

and  $k, l = 1, 2$ ,  $l \neq k$ . These equations show that the coupling coefficients  $\tilde{W}_k$  are complex and energy dependent, that  $\tilde{W}_k$  has a resonance behavior at the energy  $(\tilde{E}_k + \tilde{E}_l)/2$  with the width  $(\tilde{\Gamma}_k + \tilde{\Gamma}_l)/2$ , and that the energy dependence of the two values  $\tilde{W}_k$  and  $\tilde{\Gamma}_k$  is different in the overlapping regime. In the energy region of the resonance behavior of  $\tilde{W}_k$  caused by a neighbored resonance state  $l$ , the  $S$  matrix contains terms being nonlinear in energy.

When the widths of the two states are equal,  $\tilde{W}_k \rightarrow 0$  with  $E \rightarrow (\tilde{E}_k + \tilde{E}_l)/2$ . At large distance,  $E \gg \tilde{E}_1 + \tilde{E}_2$ , follows  $\tilde{W}_k \rightarrow \tilde{\Gamma}_k$ . In this case, the two resonance states behave as isolated ones. When the positions  $\tilde{E}_k, \tilde{E}_l$  of the two resonance states are outside of the resonance region of  $\tilde{W}_k$  and  $\tilde{W}_l$ , the resonances can also be considered, to a good approximation, as isolated, and  $\tilde{W}_k \approx \tilde{\Gamma}_k, \tilde{W}_l \approx \tilde{\Gamma}_l$ .

The nonlinear term creates some deviation in the resonance line shape from the linear Breit-Wigner one. This can be seen best in the case when the  $S$  matrix has a double pole, i.e.,  $\tilde{E}_1 = \tilde{E}_2 \equiv \tilde{E}_d$  and  $\tilde{\Gamma}_1 = \tilde{\Gamma}_2 \equiv \tilde{\Gamma}_d$ . In such a case, the  $S$  matrix (19) reads

$$\begin{aligned}
S &= 1 - 2i \frac{\tilde{W}_d}{E - \tilde{E}_d + \frac{i}{2}\tilde{\Gamma}_d} \\
&= 1 - 2i \frac{\tilde{\Gamma}_d}{E - \tilde{E}_d + \frac{i}{2}\tilde{\Gamma}_d} - \frac{\tilde{\Gamma}_d^2}{\left(E - \tilde{E}_d + \frac{i}{2}\tilde{\Gamma}_d\right)^2}. \tag{21}
\end{aligned}$$

The second term corresponds to the usual linear term, while the third term is quadratic (see Ref. [13]). The interference between these two parts has been illustrated in Ref. [14], where the cross section is shown for the case of two resonance states coupled to one channel. The energies and widths of the two resonance states are the same, creating a double pole of the  $S$  matrix. The asymmetry of the line shape of both peaks in the cross section agrees with Eq. (21). A similar picture has been obtained in, e.g., laser induced continuum structures in atoms with a double pole of the  $S$  matrix [15,16], in atom-surface collisions [17], transmission in quantum scattering systems [18], in a double barrier potential [19], a double-square-well system [20], and in a toy model for the conductance through a small quantum dot [21].

According to Eq. (20), the asymmetry of narrow resonances is usually larger than that of broad resonances: when  $\tilde{\Gamma}_1 \gg \tilde{\Gamma}_2$ , it follows  $\tilde{W}_1 \approx \tilde{\Gamma}_1$  while the corrections from  $\tilde{\Gamma}_1$  to  $\tilde{W}_2$  can mostly not be neglected. In any case, the nonlinear term in  $\tilde{W}_k$ , Eq. (20), causes a nonexponential decay of the two resonance states. Only when the line shape of a certain resonance  $k$  is of Breit-Wigner type and  $\tilde{\Gamma}_k$  is almost constant in a large energy region around  $\tilde{E}_k$ , the states  $k$  will decay according to an exponential law [13].

When the two resonance states lie at the same energy, but their widths are different, then follows from Eqs. (19) and (20) that the contributions from both resonance states annihilate each other at  $E = \tilde{E}_1 = \tilde{E}_2$ , i.e., the cross section vanishes at that energy where the two resonance states lie. This destructive interference has been traced numerically in Ref. [14] for two resonance states coupled to one channel by varying the coupling strength between the states and the continuum. When  $\tilde{\Gamma}_1 \gg \tilde{\Gamma}_2$ , the narrow resonance appears as a dip in the cross section that is determined mainly by the broad resonance. This is in accordance with Eq. (20): for  $E \rightarrow \frac{1}{2}(\tilde{E}_1 + \tilde{E}_2)$ , follows  $\tilde{W}_1 \rightarrow \tilde{\Gamma}_1$  and  $\tilde{W}_2 \rightarrow -\tilde{\Gamma}_2$ .

For illustration, the cross section calculated with two neighboring resonance states is shown in Fig. 1. The width of one of the states is fixed to  $\tilde{\Gamma}_1 = 0.05$  (in arbitrary units) while that of the other one is varied between  $\tilde{\Gamma}_2 = 0.01$  and 5.0. When  $\tilde{\Gamma}_2 \gg \tilde{\Gamma}_1$ , it is  $\tilde{\Gamma}_2 \approx \text{const}$  in the energy region of

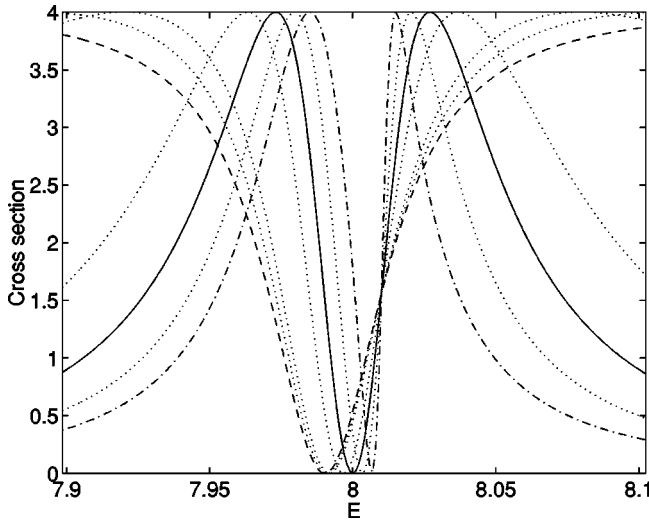


FIG. 1. Cross section with two resonance states at  $\tilde{E}_1=7.99$  and  $\tilde{E}_2=8.01$ . The width of one of the states is fixed to  $\tilde{\Gamma}_1=0.05$ , while that of the other state is varied:  $\tilde{\Gamma}_2=5.0$  (dashed curve),  $\tilde{\Gamma}_2=0.05$  (full curve), and  $\tilde{\Gamma}_2=0.01$  (dash-dotted curve). The dotted curves are calculated with  $\tilde{\Gamma}_2=1.0, 0.5, 0.1, 0.025$ , respectively. Cross section and energy are given in arbitrary units.

the narrow resonance, and the cross section shows a dip at the energy  $\tilde{E}_1$ . In this case, the broad resonance plays the role of a background for the narrow resonance. When the widths of both states are equal, the structure of the cross section is similar to that caused by Eq. (21) at the double pole of the  $S$  matrix. When  $\tilde{\Gamma}_2 < \tilde{\Gamma}_1$ , the two peaks in the cross section are no longer symmetrical in relation to the center at  $E=8$ .

The corresponding coupling coefficients  $\tilde{W}_1$  and  $\tilde{W}_2$  (Figs. 2 and 3) show a resonancelike behavior at  $E=(\tilde{E}_1+\tilde{E}_2)/2$ . While the absolute values show the same tendency for both states, their phases behave differently. The phase of the broad state is almost not influenced by the interaction with the narrow one, while the phase of the narrow state jumps by  $2\pi$  at the energy  $E=(\tilde{E}_1+\tilde{E}_2)/2$ . This is caused by the minimum of  $\text{Re}(\tilde{W}_k)$ , which is reached at  $E=(\tilde{E}_k+\tilde{E}_l)/2$ . The minimum value is  $\tilde{\Gamma}_k-\tilde{\Gamma}_l \approx \tilde{\Gamma}_k$  for the broad state, but  $-\tilde{\Gamma}_l$  for the narrow one. In both cases,  $\text{Im}(\tilde{W}_{k(l)})$  oscillates and vanishes at  $E=(\tilde{E}_k+\tilde{E}_l)/2$ . These results are in agreement with the fact that the broad resonance state plays the role of a background for the narrow resonance state.

Of special interest is the case  $\tilde{\Gamma}_1=\tilde{\Gamma}_2$ . The resonance behavior of the coupling coefficients appearing at  $E=(\tilde{E}_1+\tilde{E}_2)/2$  is independent of the distance  $|\tilde{E}_1-\tilde{E}_2|$  of the two resonance states. It reflects the properties of a double pole of the  $S$  matrix. One clearly sees the phase jump by  $\pi$  at  $E=(\tilde{E}_1+\tilde{E}_2)/2$  (Figs. 2 and 3). This energy  $E^{\text{cr}} \equiv (\tilde{E}_1+\tilde{E}_2)/2$  is the critical value at which the wave functions of the two states are exchanged when the energy is parametri-

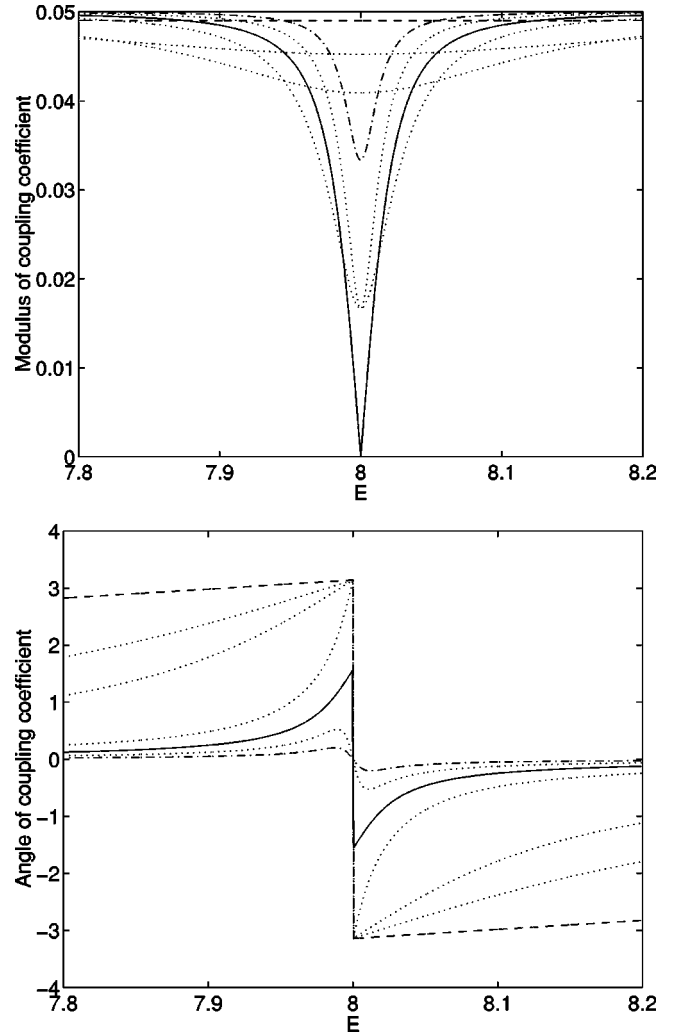


FIG. 2. Coupling coefficient  $\tilde{W}_1$  of the resonance state at  $\tilde{E}_1=7.99$ . The width is  $\tilde{\Gamma}_1=0.05$ . The position and width of the other state is as in Fig. 1.

cally varied (see Sec. IV). Here,  $\tilde{W}=0$ . However, the phase jump of  $\pi$  does not appear at every zero of the cross section, see Figs. 1–3. It follows further that the resonance behavior of the coupling coefficients plays a role only for resonance states lying near to one another.

As can be seen in Fig. 1, the interferences between the different resonance states cause, in the one-channel case, a separation of the peaks in the cross section. In this manner, the interferences may feign the existence of well-isolated resonance states in spite of their strong overlapping. An extreme case is the case with two separated peaks appearing in the cross section with a double pole of the  $S$  matrix [2,10,14] or in its neighborhood, Fig. 1.

The line shape of the peaks in the cross section is described usually by means of energy-independent Fano parameters. A recent example, is the experimentally observed narrow peak in the conductance through a quantum dot controlled by varying the strength of the magnetic field [22]. The energy-independent Fano parameters are related to a representation of the  $S$  matrix (19) with energy independent  $W'_k$

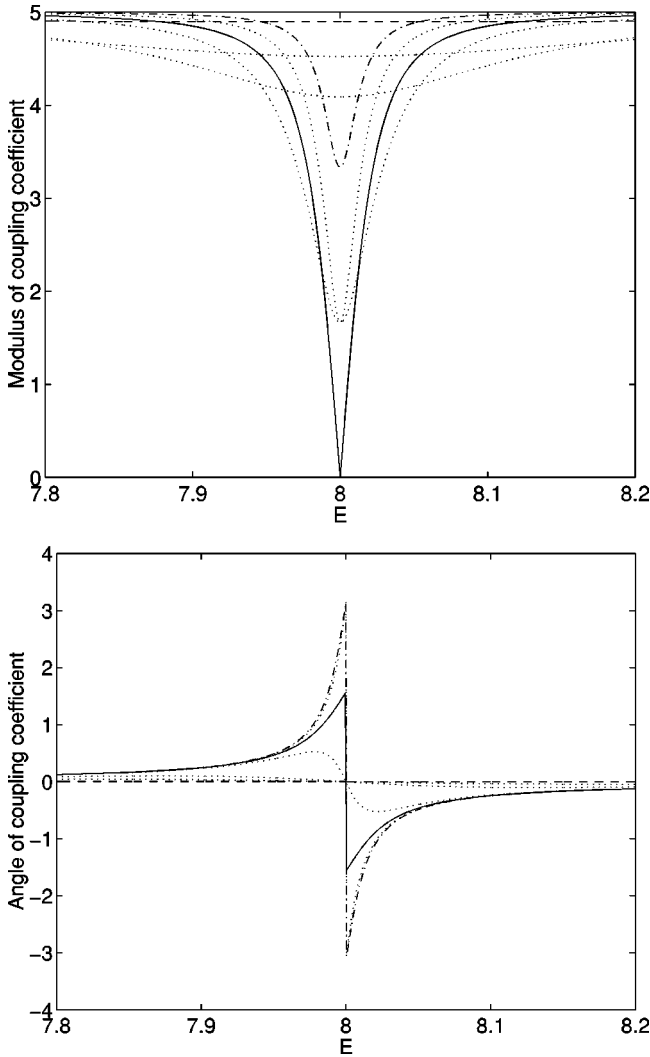


FIG. 3. Coupling coefficient  $\tilde{W}_2$  of the resonance state at  $\tilde{E}_2 = 8.01$ . The position and width of the other state as well as the width  $\tilde{\Gamma}_2$  is as in Fig. 1. In the upper part,  $|\tilde{W}_2|$  is multiplied by 1 (dashed curve), 100 (full curve), and 500 (dash-dotted curve), and by 5, 10, 50, and 200, respectively (dotted curves).

[instead of the energy dependent  $\tilde{W}_k$  in Eq. (20)]:

$$W'_k = \tilde{\Gamma}_k \left( 1 - i \frac{\tilde{\Gamma}_l}{\tilde{E}_k - \tilde{E}_l - \frac{i}{2}(\tilde{\Gamma}_k - \tilde{\Gamma}_l)} \right). \quad (22)$$

In the literature, mostly the  $W'_k$  are used since they provide the standard parametrization of the  $S$  matrix. A recent example is the analysis of the biorthogonality of resonance wave functions in the molecule  $\text{NO}_2$  [23]. The representation (22) is equivalent to Eq. (20), except in approaching a double pole of the  $S$  matrix where Eq. (22) has a singularity in contrast to Eq. (20). The  $W'_k$  lose, however, their physical meaning as the coupling matrix elements between resonance states and continuum in the overlapping regime [10]. For this reason, we will not consider them in this paper. Instead, we

will use the  $\tilde{W}_k$  that are meaningful also around double poles of the  $S$  matrix according to Eq. (21).

It is easy to generalize the study to more than two resonance states. Suppose

$$S = \prod_{n=1}^N \frac{E - \tilde{E}_n - \frac{i}{2}\tilde{\Gamma}_n}{E - \tilde{E}_n + \frac{i}{2}\tilde{\Gamma}_n} \quad (23)$$

instead of Eq. (17). In an analogy with Eqs. (19) and (20), it follows

$$S = 1 - i \sum_n \frac{\tilde{W}_n}{E - \tilde{E}_n + \frac{i}{2}\tilde{\Gamma}_n}, \quad (24)$$

with

$$\tilde{W}_n = \tilde{\Gamma}_n \left( 1 - i \sum \frac{\tilde{\Gamma}_m}{X_n + X_m} - \sum \frac{\tilde{\Gamma}_m \cdot \tilde{\Gamma}_l}{X_n X_m + X_n X_l + X_m X_l} - \dots \right) \quad (25)$$

and  $X_n \equiv E - \tilde{E}_n + (i/2)\tilde{\Gamma}_n$ . The sum in the second term of Eq. (25) is running over  $m \neq n$  and that in the third term over  $m \neq n$  and  $l \neq m, n$ . The denominator  $X_n + X_m$  of the second term is linear in  $E$ , while that of the third term,  $X_n X_m + X_n X_l + X_m X_l$ , is quadratic in  $E$ . In any case, the  $\tilde{W}_n$  depend on energy in a nontrivial manner.

As follows from Eqs. (24) and (25), the coupling coefficients at a triple pole of the  $S$  matrix are  $\tilde{W}_n = \tilde{\Gamma}_n/3$  (in contrast to  $\tilde{W}_n = 0$  at a double pole). Here, the  $S$  matrix contains terms up to third order. When one of the widths is much larger than the other ones in the three-resonance case,  $\tilde{\Gamma}_l \gg \tilde{\Gamma}_k (k=n, m)$ , it is  $\tilde{W}_l \approx \tilde{\Gamma}_l$  and  $\tilde{W}_k = -\tilde{\Gamma}_k$  when  $E = \frac{1}{2}(\tilde{E}_l + \tilde{E}_k)$ . These relations are in complete analogy with those obtained for the two-resonance case.

In Figs. 4 and 5, the cross sections with three resonance states are shown, two of which are lying symmetrically around the position of the third one at  $E = \tilde{E}_3 = 8$ , as well as the coupling coefficients  $\tilde{W}_3$ . The different curves in Fig. 4 are obtained by varying the width  $\tilde{\Gamma}_3$  between 0.05 and 5. In the first case, the widths of all three states are equal, while in the other cases, the middle state overlaps the narrower ones. When  $\tilde{\Gamma}_3 \gg \tilde{\Gamma}_k (k=1,2)$ , the broad state can be considered as a “background” for the other two: these appear as dips in the cross section. This can be seen better in Fig. 6 where one broad resonance state ( $\tilde{\Gamma}_3 = 3.0$ ) is shown that overlaps two narrow ones ( $\tilde{\Gamma}_1 = \tilde{\Gamma}_2 = 0.05$ ). In both cases, a peak appears in the middle of the spectrum at  $E = 8$  in contrast to the two-resonance case, Fig. 1. In Fig. 5, the widths of all three states are kept constant, while the distance between them is

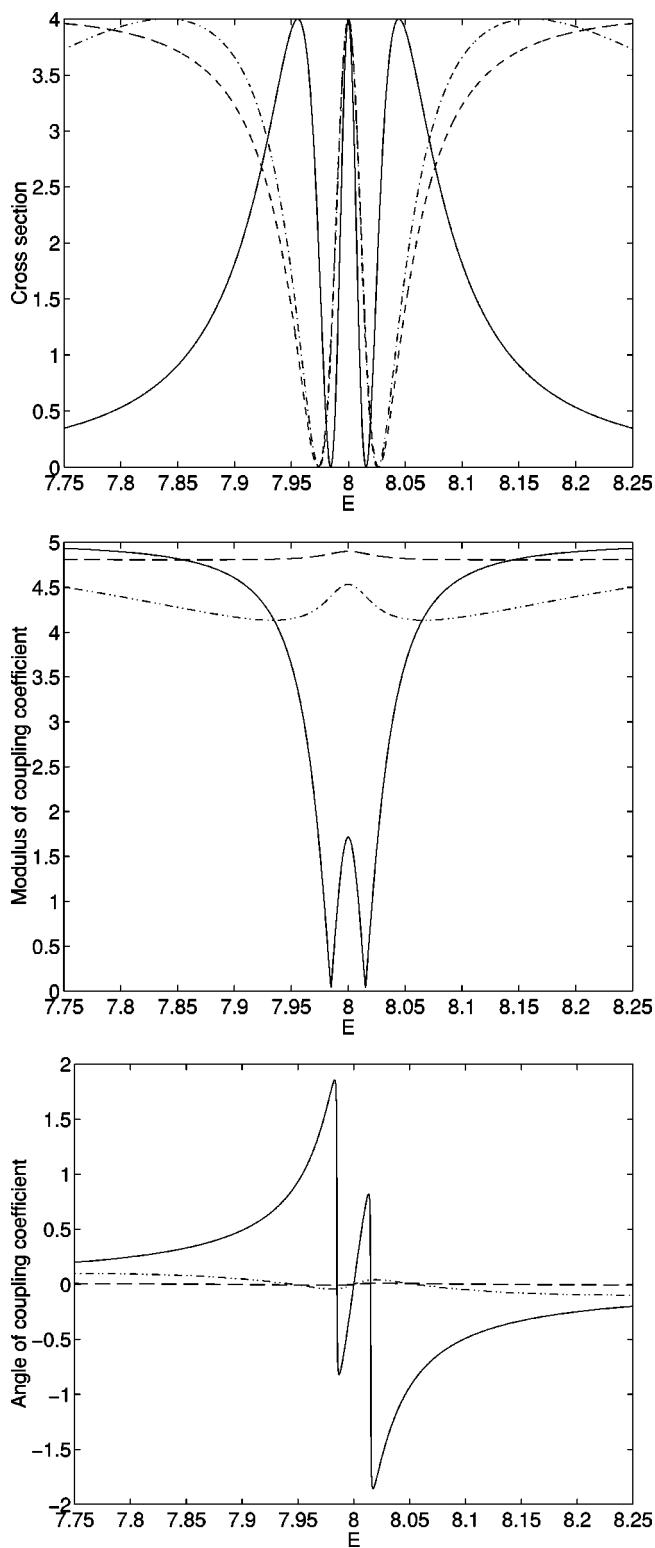


FIG. 4. Cross section (top) with three resonance states at  $\tilde{E}_1 = 7.99$ ,  $\tilde{E}_2 = 8.01$ ,  $\tilde{E}_3 = 8.0$  and  $\tilde{\Gamma}_1 = \tilde{\Gamma}_2 = 0.05$ ,  $\tilde{\Gamma}_3 = 0.05$  (full curve),  $\tilde{\Gamma}_3 = 1.0$  (dash-dotted curve), and  $\tilde{\Gamma}_3 = 5.0$  (dashed curve). Coupling coefficient (middle and bottom)  $\tilde{W}_3$  of the resonance state in the middle of the spectrum.  $|\tilde{W}_3|$  is multiplied by 100 (full curve), 5 (dash-dotted curve), and 1 (dashed curve). Cross section and energy are given in arbitrary units.

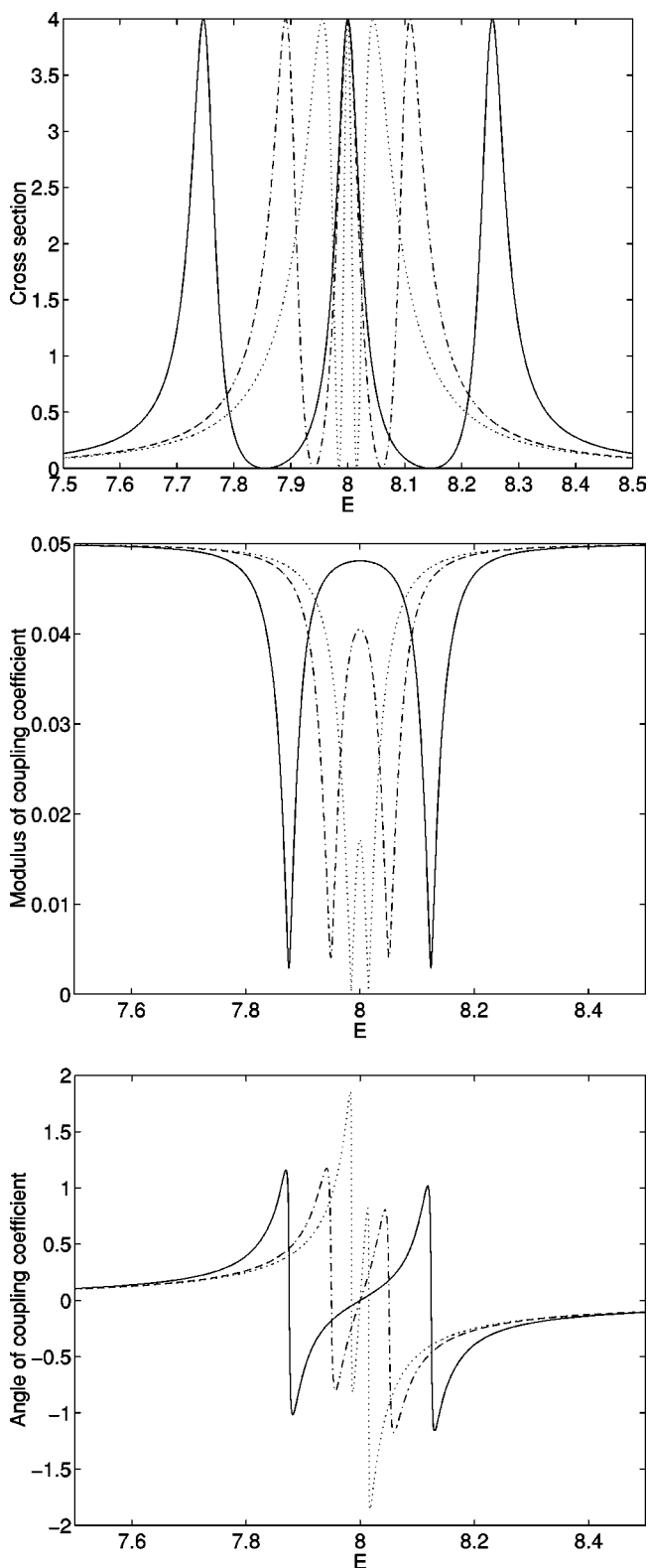


FIG. 5. Cross section (top) with three resonance states of widths  $\tilde{\Gamma}_1 = \tilde{\Gamma}_2 = \tilde{\Gamma}_3 = 0.05$  at  $\tilde{E}_1 = 7.99$ ,  $\tilde{E}_2 = 8.01$ ,  $\tilde{E}_3 = 8.0$  (dotted curve);  $\tilde{E}_1 = 7.9$ ,  $\tilde{E}_2 = 8.1$ ,  $\tilde{E}_3 = 8.0$  (dash-dotted curve); and  $\tilde{E}_1 = 7.75$ ,  $\tilde{E}_2 = 8.25$ ,  $\tilde{E}_3 = 8.0$  (full curve). Coupling coefficient  $\tilde{W}_3$  (middle and bottom) of the resonance state in the middle of the spectrum. Cross section and energy are given in arbitrary units.

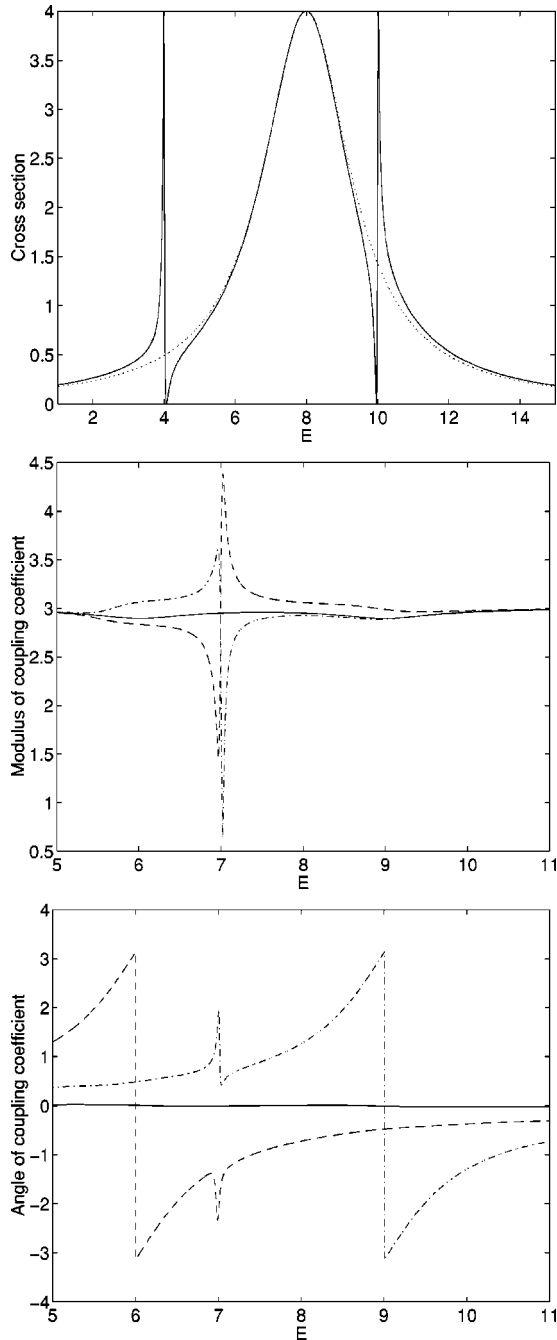


FIG. 6. Cross section (top) with one resonance state of width  $\tilde{\Gamma}_3=3.0$  at  $\tilde{E}_3=8.0$  (dotted curve) and with two additional resonance states of widths  $\tilde{\Gamma}_1=\tilde{\Gamma}_2=0.05$  at  $\tilde{E}_1=4.0$  and  $\tilde{E}_2=10.0$ , respectively (full curve). Coupling coefficients (middle and bottom)  $\tilde{W}_1$  (dashed),  $\tilde{W}_2$  (dash-dotted), and  $\tilde{W}_3$  (full curve) of the three resonance states.  $|\tilde{W}_1|$  and  $|\tilde{W}_2|$  are multiplied by 60. Cross section and energy are given in arbitrary units. Note the different energy scales for the cross section and the coupling coefficients.

varied. Although the peaks in the cross section seem to be well isolated from one another for  $(\tilde{E}_k - \tilde{E}_{k\pm 1})/(\tilde{\Gamma}_k + \tilde{\Gamma}_{k\pm 1}) = 2.5$  (full curve), the interferences between the resonance states are not vanishing.

Interesting are again the phase jumps of the coupling co-

efficients  $\tilde{W}_3$  at the critical values of the energy  $E^{\text{cr}} = (\tilde{E}_k + \tilde{E}_3)/2$ ;  $k=1,2$ . They are mostly smaller than those of  $\tilde{W}_1$  and  $\tilde{W}_2$  (not shown). The influence of a broad resonance state on the coupling coefficients of narrow ones is illustrated in Figs. 6 and 7 with the state 3, being, respectively, much broader and much narrower than the states 1 and 2. At the energies 6 and 9, the states 1 and 2, respectively, interact with the state 3 while the interference picture at the energy 7 is caused by the two states 1 and 2 with equal widths. The phase jump of  $\pi$  at this energy (Fig. 7) is reduced in the presence of the broad resonance state (Fig. 6). Also,  $|\tilde{W}_1|$  and  $|\tilde{W}_2|$  differ in the two cases without and with a broad state.

Measurements of phase and magnitude of the reflection and transmission coefficients of a quantum dot are performed in Ref. [24]. As a result, the phases of the dot's transmission and reflection coefficients change abruptly by about  $\pi$  at some energy in the resonance peak. The phase changes are very similar to those observed in the present calculations for the  $\tilde{W}$  in the one-channel case (see the figures). As discussed above, they are related to the unitarity of the  $S$  matrix in the overlapping regime. The results are expected to be similar for the case with more channels (or terminals) since, as will be shown in Sec. IV, they are characteristic of the intrinsic wave functions  $\tilde{\Phi}_k$  and  $\tilde{\Phi}_k^{\text{ch}}$ , respectively, of the system.

In the consideration, presented in this section, the  $\tilde{E}_k$  and  $\tilde{\Gamma}_k$  are assumed to be independent of the energy. This is, mostly, a good approximation in the energy range of the resonance state  $k$ . In any case, the energy dependence of the coupling coefficients  $\tilde{W}_k$  arises primarily from their resonance behavior caused by a neighboring resonance state, Eq. (20). It may be influenced, of course, by the energy dependence of  $\tilde{E}_k$  and  $\tilde{\Gamma}_k$ , especially when the levels repel or attract each other by varying a certain parameter.

#### IV. WAVE FUNCTIONS NEAR AVOIDED LEVEL CROSSINGS IN THE COMPLEX PLANE

The coupling coefficients between system and continuum are defined by  $(\tilde{\gamma}_k^c)^2$ , Eq. (5). Their energy dependence and phase are determined, in the one-channel case, by the energy dependence and phase of the  $(\tilde{\Phi}_k)^2$  (after removing the common phase and energy dependence caused by the  $\xi_E^c$ ). Much can, therefore, be learned on the behavior of the coupling coefficients between system and environment from a study of the wave functions  $\tilde{\Phi}_k$ .

Characteristic of the overlapping regime are avoided level crossings in the complex plane. At an avoided level crossing, the wave functions of the two crossing states are exchanged. This fact is very well known for a long time for discrete states (Landau-Zener effect). It holds also for resonance states in the adiabatic limit [2]. The difference between avoided crossings of discrete and resonance states consists mainly in the fact that resonance states may cross in the complex plane even when the interaction between them is nonvanishing and, furthermore, that the crossing may lead

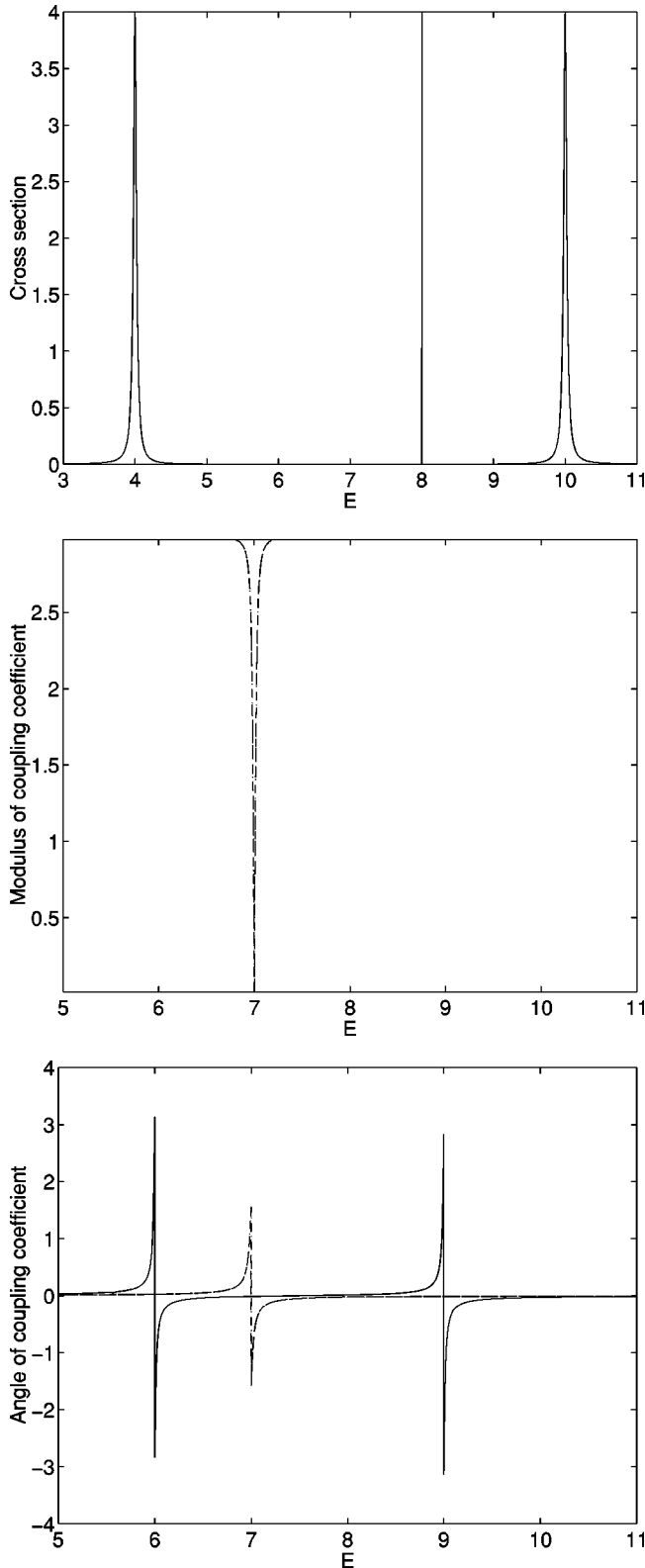


FIG. 7. The same as Fig. 6, but  $\tilde{\Gamma}_3 = 3 \times 10^{-5}$ .

not only to level repulsion but also to level attraction. While level repulsion is accompanied by the tendency to equilibrate the widths of the resonance states, level attraction is accompanied by the formation of different time scales in the system.

The avoided level crossing of resonance states can be traced back to a branch point in the complex plane [25]. When the conditions for crossing of the two levels are fulfilled, the branch point in the complex plane is nothing else than a double pole of the  $S$  matrix (see also Ref. [26]). In any case, the wave functions of the two levels are exchanged at the critical value of the parameter at which the two levels avoid crossing (or cross in one point). Here, either the widths or the energies (positions) of both states are equal. In the first case, the avoided crossing happens, as for discrete states, in the energies of the resonance states traced as a function of the considered parameter. In the second case, however, it appears in their widths.

Further studies have shown that the wave functions at the critical value  $a^{\text{cr}}$  of the parameter  $a$  are exchanged according to

$$\tilde{\Phi}_k \rightarrow \pm i \tilde{\Phi}_l, \quad (26)$$

where  $k$  and  $l$  are the two crossing states. This relation has been obtained analytically [25] as well as in a numerical study of atoms in a laser field [16]. It is related to nonlinear terms that appear in the Schrödinger equation due to the biorthogonality of the eigenfunctions of the effective Hamiltonian  $\mathcal{H}$ . At  $a^{\text{cr}}$ , the sign of the imaginary part of the wave function  $\tilde{\Phi}_k$  jumps from  $+$  to  $-$  (or opposite) even when the two states avoid crossing and  $A_k \equiv |\tilde{\Phi}_k|$  remains finite [25]. This means, in a certain parameter range  $a^{\text{min}} \leq a^{\text{cr}} \leq a^{\text{max}}$ , the wave functions of the two states  $k$  and  $l \neq k$  are mixed,

$$\tilde{\Phi}_k^{\text{ch}} = \beta_k \tilde{\Phi}_k \pm i \beta_l \tilde{\Phi}_l. \quad (27)$$

The wave functions  $\tilde{\Phi}_k^{\text{ch}}$  change smoothly (without any jump of the sign of their components)

$$\begin{aligned} &\text{from } \beta_k \rightarrow \pm 1, \beta_l \rightarrow 0 \quad \text{at } a \rightarrow a^{\text{min}} < a^{\text{cr}} \\ &\text{to } \beta_k \rightarrow 0, \beta_l \rightarrow \pm 1 \quad \text{at } a \rightarrow a^{\text{max}} > a^{\text{cr}}. \end{aligned} \quad (28)$$

The values  $a^{\text{min}}$  and  $a^{\text{max}}$  may be quite different from one another [25]. Only in the case where the avoided level crossing shrinks to one point, being the double pole of the  $S$  matrix,  $\beta_k = 0$  or  $\pm 1$  for all  $a$  but  $a^{\text{cr}}$ . In any case, the two wave functions  $(1/\sqrt{2})(\tilde{\Phi}_k \pm i \tilde{\Phi}_l)$  and  $(1/\sqrt{2})(\tilde{\Phi}_l \mp i \tilde{\Phi}_k)$  remain unchanged at  $a = a^{\text{cr}}$  under the exchange (26).

Hence, in the parameter range  $a^{\text{min}} < a < a^{\text{max}}$ , the wave functions of the two states are  $\tilde{\Phi}_k^{\text{ch}}$ , but not  $\tilde{\Phi}_k$  ( $k=1,2$ ). The two wave functions are restored, after the exchange at  $a^{\text{cr}}$ , only at  $a \geq a^{\text{max}}$ . In other words, using the representation

$$\tilde{\Phi}_k^{\text{ch}} = |\tilde{\Phi}_k^{\text{ch}}| e^{i\theta_k}, \quad (29)$$

$\theta_k$  depends on  $a$  when  $a^{\text{min}} < a < a^{\text{max}}$ . Beyond this parameter area,  $\theta_k$  depends on  $a$  much weaker (if at all). After removing a common phase factor, it follows from Eq. (28) for an avoided level crossing near the double pole:  $\theta_k \rightarrow \pm \pi/4$  and

$\pm 3\pi/4$ , respectively, in approaching  $a^{cr}$  and  $\theta_k \rightarrow 0$  or  $\pi$  in approaching  $a^{\min}$  or  $a^{\max}$ . At  $a^{cr}$ , the states are chiral.

The comparison of Eq. (26) with the experimental data obtained from microwave cavities has been discussed in detail in Ref. [27]. All the data published in Refs. [28,29] for the case of two levels of the system that are well isolated from the other ones, can be explained by means of Eq. (26). Some chirality appears: left and right turns around the double pole of the  $S$  matrix with  $\beta_k = \beta_l$  are different from one another according to Eqs. (27) and (28).

Phase changes of the wave functions in the conductance through a microwave cavity have been considered in Refs. [30,31]. The question is studied to what extent the transport through the cavity changes the structure of its internal wave functions. It is demonstrated theoretically as well as experimentally [30] that the standing waves of the original cavity are transformed more or less completely into running waves propagating from the entrance antenna to different exit ports. This is expressed by the two limiting cases: (i) the real and imaginary parts of the wave functions are strongly correlated, and (ii) they are completely uncorrelated. In the last case, the real and imaginary parts of the wave functions of the resonance states evolve independently in the open microwave cavity.

In Ref. [32], the phase difference between two modes has been measured in a cavity composed of two almost identical semicircular parts. The two modes are each localized in one of the semicircular parts of the cavity and are excited separately by appropriately positioned dipole antennas. The corresponding two eigenvalues are well separated from all the other ones. By varying two parameters (designed here together by  $a$ ) of the cavity, their avoided crossing in the complex plane to a (almost) true crossing can be traced. Furthermore, the eigenfunctions are studied by mapping the distributions of the electric field. Finally, the phase difference  $\Delta = \theta_k - \theta_l$  between the antennas has been found for different distances of  $a$  from the critical value  $a^{cr}$ . The results obtained in the experiment [32] are  $\Delta \rightarrow \pi/2$  for  $a \rightarrow a^{cr}$  and  $\Delta = \pi$  for  $a$  beyond the range  $a^{\min} < a < a^{\max}$ . They agree with Eqs. (27) and (28) by using the representation (29) [33].

According to Eq. (5), the phase of the coupling coefficients  $(\tilde{\gamma}_k^c)^2$  is determined by that of  $(\tilde{\Phi}_k)^2$ . Considered as a function of a certain parameter, the phases of both expressions vary, in the one-channel case, in the same manner. Since the parameter may be also the energy of the system [2], the phase of the  $(\tilde{\gamma}_k^c)^2$  varies generically with the energy in the same manner as the phase of the  $(\tilde{\Phi}_k)^2$ . The results discussed above are in full agreement with those following immediately from the unitarity of the  $S$  matrix, Figs. 2–7. Even the jumps by  $\pi$  appearing in the phases of the coupling coefficients  $\tilde{W}$  in Figs. 2, 3, and 7 can be explained by Eqs. (26) and (27). In other words, Eqs. (26)–(28) coincide with the postulation of the unitarity of the  $S$  matrix. In any case, nonlinearities are responsible for the energy dependence of the coupling coefficients between system and continuum.

In realistic systems, mostly more than two resonance states are coming close to one another, i.e., avoided crossings

of more than two resonance states take place in the parameter range  $a^{\min} < a < a^{\max}$ . As an extreme case, the branch point in the complex plane may be a multiple pole of the  $S$  matrix. The relation between the different wave functions is, in such a case, more complicated than that for two states where the wave functions of only two resonance states are exchanged according to Eq. (26), mixed in the range  $a^{\min} < a < a^{\max}$  and restored beyond this range. Such a situation is studied experimentally [28] as well as theoretically in different approaches [4,25,34,35], compare also Figs. 2 and 3 for two resonance states with Figs. 4 and 5 for three resonance states as well as Fig. 6 with Fig. 7.

## V. CONCLUDING REMARKS

The resonance phenomena are described well by two ingredients also at high level density. The first ingredient is the effective Hamiltonian  $\mathcal{H}$  that contains all the basic structure information involved in the Hamiltonian  $H$ , i.e., in the Hamiltonian of the corresponding closed system with discrete eigenstates. Moreover,  $\mathcal{H}$  contains the coupling matrix elements  $W_k^{cc'}$  between discrete states and continuum which account for the changes of the system under the influence of its coupling to the continuum. These matrix elements are responsible for the non-Hermiticity of  $\mathcal{H}$  and its complex eigenvalues which transfer the discrete states into resonance states and determine not only their positions but also their (finite) lifetimes.

The second ingredient is the unitarity of the  $S$  matrix that has to be fulfilled in all calculations of resonance phenomena. The unitarity of the  $S$  matrix causes a nontrivial energy dependence of the coupling matrix elements  $\tilde{W}_k^{cc'}$  between resonance states and continuum. This energy dependence becomes decisive in the overlapping regime even in the case the lifetimes of the overlapping states are very different from one another and the different long-lived states seem to be well-isolated from one another. It is taken into account in the unified description of structure and reaction aspects since any statistical or perturbative assumptions are avoided in solving the basic equation (1). The unitarity of the  $S$  matrix influences also the phases of the wave functions of the resonance states that change generically in approaching avoided level crossings in the complex plane.

In the nonoverlapping regime, both ingredients are fulfilled in almost all theoretical approaches. Here, the wave functions and positions of the resonance states are described, to a good approximation, by the wave functions and positions of the discrete states of the corresponding closed system. The coupling matrix elements between system and continuum can be calculated by means of the wave functions of the discrete states. They are energy independent, to a good approximation.

In the overlapping regime, however, with many avoided level crossings, the wave functions of the resonance states suffer phase changes. Furthermore, the coupling coefficients of the resonance states to the continuum show a resonance-like behavior caused by the interaction with a neighbored resonance state. Both effects are described by nonlinear terms appearing in the Schrödinger equation and the  $S$  matrix, respectively. They are related to one another and cannot be neglected at high level density.

As a conclusion of these results, the coupling of a quan-

tum system to the environment may change its properties. The changes are small as long as the coupling strength between system and environment is smaller than the distance between the individual states of the unperturbed system, i.e., smaller than the distance between the eigenstates of the Hamiltonian  $H$ . The changes can, however, not be neglected when the coupling to the continuum is of the same order of magnitude as the level distance or larger. In such a case, the changes can be described neither by perturbation theory nor by introducing statistical assumptions for the level distribution. Here, nonlinear effects become important which cause a redistribution of the spectroscopic properties of the system and, consequently, changes of its features.

Under the influence of the coupling to the continuum, not only level repulsion but also level attraction may appear. The first case is accompanied by the tendency to form a uniform

time scale for the system while different time scales are formed in the second case. The formation of different time scales in an open quantum system, which is accompanied by level attraction, is accompanied also by the appearance of a nontrivial energy and phase dependence of the coupling coefficients  $\tilde{W}$ . The use of an effective non-Hermitian Hamiltonian operator in describing scattering processes in the overlapping regime is therefore meaningful only when, at the same time, the energy dependence of the  $\tilde{W}$  is considered.

#### ACKNOWLEDGMENT

I am indebted to A. I. Magunov, N. Moiseyev, and E. Persson for valuable discussions and to H. Schomerus for a critical reading of the manuscript.

- 
- [1] H. Feshbach, *Ann. Phys. (N.Y.)* **5**, 357 (1958); **19**, 287 (1962).  
 [2] J. Okołowicz, M. Płoszajczak, and I. Rotter, *Phys. Rep.* **374**, 271 (2003).  
 [3] Y.V. Fyodorov and B. Mehlige, *Phys. Rev. E* **66**, 045202 (2002); Y.V. Fyodorov and H.J. Sommers, *J. Phys. A* **36**, 3303 (2003).  
 [4] C. Jung, M. Müller, and I. Rotter, *Phys. Rev. E* **60**, 114 (1999).  
 [5] T. Guhr, A. Müller-Groeling, and H.A. Weidenmüller, *Phys. Rep.* **299**, 190 (1998).  
 [6] K. Pichugin, H. Schanz, and P. Šeba, *Phys. Rev. E* **64**, 056227 (2001).  
 [7] Y.V. Fyodorov and H.J. Sommers, *J. Math. Phys.* **38**, 1918 (1997).  
 [8] F.M. Dittes, *Phys. Rep.* **339**, 215 (2000).  
 [9] D.V. Savin, V.V. Sokolov, and H.J. Sommers, *Phys. Rev. E* **67**, 026215 (2003).  
 [10] A. I. Magunov, I. Rotter, and S. I. Strakhova, e-print quant-ph/0305064.  
 [11] I. Rotter, *Rep. Prog. Phys.* **54**, 635 (1991).  
 [12] E. Persson, I. Rotter, H.J. Stöckmann, and M. Barth, *Phys. Rev. Lett.* **85**, 2478 (2000); H.J. Stöckmann, E. Persson, Y.H. Kim, M. Barth, U. Kuhl, and I. Rotter, *Phys. Rev. E* **65**, 066211 (2002).  
 [13] R. G. Newton, *Scattering Theory of Waves and Particles* (Springer-Verlag, New York, 1982).  
 [14] M. Müller, F.M. Dittes, W. Iskra, and I. Rotter, *Phys. Rev. E* **52**, 5961 (1995).  
 [15] C.J. Joachain, M. Dörr, and N. Kylstra, *Adv. At., Mol., Opt. Phys.* **42**, 225 (2000).  
 [16] A.I. Magunov, I. Rotter, and S.I. Strakhova, *J. Phys. B* **32**, 1669 (1999); **34**, 29 (2001).  
 [17] S.D. Bosanac, *Phys. Rev. A* **30**, 142 (1984); **30**, 148 (1984).  
 [18] T. Taniguchi and M. Büttiker, *Phys. Rev. B* **60**, 13 814 (1999).  
 [19] E. Hernández, A. Jáuregui and A. Mondragón, *J. Phys. A* **33**, 4507 (2000).  
 [20] W. Vanroose, *Phys. Rev. A* **64**, 062708 (2001).  
 [21] A. Silva, Y. Oreg and Y. Gefen, *Phys. Rev. B* **66**, 195316 (2002).  
 [22] V. Madhavan, W. Chen, T. Jamneala, M.F. Crommie, and N.S. Wingreen, *Science* **280**, 567 (1998); J. Göres, D. Goldhaber-Gordon, S. Heemeyer, M.A. Kastner, H. Shtrikman, D. Mahalu, and U. Meirav, *Phys. Rev. B* **62**, 2188 (2000); K. Kobayashi, H. Aikawa, S. Katsumoto, and Y. Iye, *Phys. Rev. Lett.* **88**, 256806 (2002).  
 [23] S.Yu. Grebenshchikov, *J. Phys. Chem. A* **104**, 10409 (2000).  
 [24] A. Yacoby, M. Heiblum, D. Mahalu, and H. Shtrikman, *Phys. Rev. Lett.* **74**, 4047 (1995); E. Buks, R. Schuster, M. Heiblum, D. Mahalu, V. Umansky, and H. Shtrikman, *ibid.* **77**, 4664 (1996); R. Schuster, E. Buks, M. Heiblum, D. Mahalu, V. Umansky, and H. Shtrikman, *Nature (London)* **385**, 417 (1997).  
 [25] I. Rotter, *Phys. Rev. E* **64**, 036213 (2001); *Phys. Rev. C* **64**, 034301 (2001).  
 [26] N. Moiseyev, *Phys. Rep.* **302**, 211 (1998).  
 [27] I. Rotter, *Phys. Rev. E* **65**, 026217 (2002); **67**, 026204 (2003).  
 [28] H.M. Lauber, P. Weidenhammer, and D. Dubbers, *Phys. Rev. Lett.* **72**, 1004 (1994).  
 [29] C. Dembowski, H.D. Gräf, H.L. Harney, A. Heine, W.D. Heiss, H. Rehfeld, and A. Richter, *Phys. Rev. Lett.* **86**, 787 (2001).  
 [30] P. Šeba, F. Haake, M. Kús, M. Barth, U. Kuhl, and H.J. Stöckmann, *Phys. Rev. E* **56**, 2680 (1997).  
 [31] H. Ishio, A.I. Saichev, A.F. Sadreev, and K.F. Berggren, *Phys. Rev. E* **64**, 056208 (2001).  
 [32] C. Dembowski, B. Dietz, H.D. Gräf, H.L. Harney, A. Heine, W.D. Heiss, and A. Richter, *Phys. Rev. Lett.* **90**, 034101 (2003).  
 [33] The interpretation of the experimental data given here on the basis of Eqs. (27) and (28) differs from that given in Ref. [32]. The authors of Ref. [32] consider the reduction of the dimension of the Hilbert space at  $a = a^{ct}$  ("defect of the Hilbert space") which is caused by the coalescence of two eigenmodes. In the case studied, the number of states is assumed to be reduced from 2 to 1 at  $a^{ct}$ . This reduction of the number of states is suggested to be responsible for the reduction of  $\Delta$  from  $\pi$  to  $\pi/2$  at  $a^{ct}$ . In difference to that interpretation, the reduction of  $\Delta$  from  $\pi$  to  $\pi/2$  is caused, in the formalism given in the present paper, first of all by the different degree of mixing of the two states according to Eq. (28). It takes place

smoothly in a certain region around  $a^{cr}$  in agreement with the experimental data published in Ref. [32]. In the present formalism, diabolic points and exceptional points are related to one another. Nevertheless, they are not the same in contrast to the statement given in reference [5] of [32].

- [34] F. Pistolesi and N. Manini, Phys. Rev. Lett. **85**, 1585 (2000); N. Manini and F. Pistolesi, *ibid.* **85**, 3067 (2000).
- [35] E. Narevicius and N. Moiseyev, Phys. Rev. Lett. **84**, 1681 (2000); J. Chem. Phys. **113**, 6088 (2000).